

1 **An Artificial Neural Network to predict the hydrological response of a forest after wildfire**
2 **and soil treatments**

3

4 Demetrio Antonio Zema^(1,*), Manuel Esteban Lucas-Borja⁽²⁾, Lidia Fotia⁽³⁾, Domenico Rosaci⁽⁴⁾,
5 Giuseppe M. L. Sarnè⁽³⁾, Santo Marcello Zimbone⁽¹⁾

6

7 ⁽¹⁾ *Department AGRARIA, University "Mediterranea" of Reggio Calabria, Località Feo di Vito, I-*
8 *89122 Reggio Calabria (Italy)*

9 ⁽²⁾ *Departamento de Ciencia y Tecnología Agroforestal y Genética, Universidad de Castilla La*
10 *Mancha, Campus Universitario s/n, C.P. 02071, Albacete (Spain)*

11 ⁽³⁾ *Department DICEAM, University "Mediterranea" of Reggio Calabria, Località Feo di Vito, I-*
12 *89122 Reggio Calabria (Italy)*

13 ⁽⁴⁾ *Department DIIES, University "Mediterranea" of Reggio Calabria, Località Feo di Vito, I-89122*
14 *Reggio Calabria (Italy)*

15

16 * corresponding author, dzema@unirc.it

17

18 **ABSTRACT**

19

20 Accurate predictions of surface runoff and soil erosion after wildfire help land managers adopt the
21 most suitable actions to mitigate post-fire land degradation and rehabilitation planning. The use of
22 the Artificial Neural Networks (ANNs) is advisable as hydrological prediction tool, given their
23 lower requirement of input information compared to the traditional hydrological models.

24 This study proposes an ANN model, purposely prepared for forest areas of the semi-arid
25 Mediterranean environments. The ANN hydrological prediction capability in non-burned, burned
26 by wildfire, and burned and then treated soils has been verified at the plot scale in pine forests of

27 South-Eastern Spain. Runoff and soil loss were much higher than non-burned soils (assumed as
28 control), but mulch application was effective to control runoff and soil erosion in burned plots.
29 Moreover, logging did not affect the hydrological response of these soils. The model gave very
30 accurate runoff and erosion predictions in burned and non-burned soils as well as for all soil
31 treatments (mulching and/or logging or not), with only one exception (that is, in the condition with
32 the combination of treatments which gave the worst performance, burning, mulching and logging),
33 as shown by the exceptionally high model efficiency and coefficients of determination. Although
34 further experimental tests are needed to validate the ANN applicability to the burned forests of the
35 semi-arid conditions and other ecosystems, the use of ANN can be suggested to landscape planners
36 as decision support system for the integrated assessment and management of forests.

37

38 **KEYWORDS:** Artificial Intelligence; hydrological modelling; surface runoff; erosion; mulching;
39 logging.

40

41 **1. INTRODUCTION**

42

43 The increased frequency and severity of summer droughts due to the forecasted global warming are
44 expected to lead to an important increase in the severity and recurrence of wildfires, which may
45 affect processes and properties of forest soils (Certini, 2014). Forest fire generates a chain of
46 physico-chemical and biological processes, whose effects influence the entire ecosystem. One of the
47 most threatening effect of forest fire soil is the change in its post-fire hydrological response, strictly
48 linked to fire severity (Morales et al., 2000; Benavides-Solorio and MacDonald, 2005; Robichaud et
49 al., 2007). In other words, the more severe the fire is, the greater is the susceptibility to surface
50 runoff and soil erosion. More specifically, key factors enhancing runoff and soil loss are the
51 reduction in infiltration, increase in water repellence, destruction of vegetal cover, and loss of soil
52 organic matter (Larsen et al., 2009; Neary et al., 2005). The changes in soil hydrology induced by

53 wildfire are of high importance particularly in Mediterranean areas, where the infiltration-excess
54 mechanism dominates runoff and erosion generation (Plaza-Alvarez et al., 2019). In such an
55 environmental context, intense storm events in autumn and hot summers with drought risks make
56 these zones prone to post-fire erosion and wildfire occurrence, respectively (Shakesby, 2011).
57 Therefore, the post-fire changes in soil hydrology are the key to understand the post-fire restoration;
58 however, the number of the studies analysing the post-fire effects on soils at multi-year scale is
59 larger than short-term research (few months after fire).

60 Moreover, it is very important to understand the hydrological effects (that is, the potential reduction
61 of surface runoff and erosion) of the post-fire stabilization and rehabilitation treatments, used to
62 mitigate the short-term effects on soil degradation (Robichaud et al., 2000). Among these treatments,
63 emergency post-fire activities for soil stabilization, such as mulching, are recommended in areas
64 burned by wildfire to minimize overland flow and erosion risk (Vega et al., 2014). In any case, the
65 need of a better understanding and prediction of the hydrological effects of wildfire fires has created
66 a strong demand for tool able to simulate post-fire runoff and soil loss (Moody et al., 2013).
67 Accurate predictions of water and sediment flows after fire help land managers in the adoption of
68 the most suitable actions to mitigate post-fire land degradation and rehabilitation planning (Moody
69 et al., 2013). With regards to post-fire erosion modelling, literature reports simple empirical models
70 (such as the Universal Soil Loss Equation, USLE, and its revised version, the RUSLE model), semi-
71 empirical models (e.g., the revised Morgan–Morgan–Finney model, Morgan 2001), and physically-
72 based models (for instance, the Water Erosion Prediction Project (WEPP)). However, many
73 hydrological models were developed for agricultural regions, and thus such models may find
74 limited applicability in burned conditions of the Mediterranean ecosystems (Esteves et al., 2012;
75 Vieira et al., 2014; 2018).

76 In the last two decades data-driven models, such as the Artificial Neural Networks (ANNs), had an
77 increasing popularity for estimating and forecasting water resources (Hsu et al., 1995; Riad et al.,
78 2004; Sharma and Tiwari, 2009). The ANNs have been applied to complex, dynamic and highly

79 non-linear systems (Hsu et al., 1995), and in situations where the input is incomplete or ambiguous,
80 since they can analyze multi-source dataset (Tokar and Johnson, 1999). The main advantage of the
81 ANNs over traditional methods is the lower requirements of information about the complex nature
82 of the underlying process that are instead described in a mathematical closed form (Sudheer et al.,
83 2002). Furthermore, ANNs can generalise relationships also from a small dataset, but remain more
84 or less robust when noisy or missing inputs are present and can work also in changing environments
85 (Dawson and Wilby, 1998). ANNs learn from the analysis of the available input data and do not
86 require reprogramming, but they must be trained, optimized and tested (Gholam et al., 2018).
87 ANNs have been extensively used also for rainfall-runoff modeling, flood predictions, reservoir
88 operations, routing of polluting compounds (ASCE, 2000). For instance, ANNs have been used for
89 modelling the rainfall-runoff relationships in small to large watersheds of United States (Hsu et al.,
90 1995), United Kingdom (Dawson and Wilby, 1998), India (Sudheer et al., 2002; Sharma and
91 Tiwari, 2009), Morocco (Riad et al., 2004), Albaradeya et al., 2011 (in Palestinian territories) and,
92 more recently, in Australia (Asadi et al., 2019). Also, soil erosion was predicted using ANNs at
93 both plot scale (Licznar and Nearing, 2003, and Kim and Gilley, 2008, in USA; Albaradeya et al.,
94 2011, in Palestinian territories) and watershed scale (e.g., Gholami et al., 2018, in Iran). Moreover,
95 Yusof et al. (2014) used ANNs to predict the soil erodibility factor of the USLE equation using 74
96 samples of Malaysia soils.

97 However, only a few studies have analysed the ANN performance in soil erosion modelling
98 (Gholami et al., 2018) and, even, ANN has not been used for hydrological predictions in burned
99 soils. Modelling soil erosion and runoff after wildfires using ANNs may be a novel approach that
100 could be of help to better understand and predict fire-induced effects after fire.

101 To fill this gap, this study provides an ANN model, purposely prepared for pine forest areas of the
102 semi-arid Mediterranean environments, and verifies its hydrological prediction capability in non-
103 burned, burned by wildfire, and burned and then treated soils. More specifically, surface runoff and
104 soil loss were firstly measured in *i*) unburned plots (assumed as control); *ii*) plots subjected to a

105 wildfire and not rehabilitated with any post-fire measures; *iii*) plots subjected to fire and treated
106 with mulching throughout one year. Based on these observations, the ANN model is calibrated and
107 its performance in estimating surface runoff and soil loss at the event scale is evaluated under the
108 peculiar climatic conditions and forest management.

109

110 **2. THEORETICAL APPROACH ABOUT THE ARTIFICIAL NEURAL NETWORKS**

111

112 In this work a standard feedforward neural network has been used to simulate the hydrological
113 response of the experimental plots. A standard feedforward neural network (Haykin, 1994) is
114 composed by a set of N nodes N and a set of M arcs A . The nodes are partitioned into L groups,
115 called *layers*, with $L > 2$. The first layer is a set of I input nodes NI called *input layer*; then, there
116 are $L-2$ *hidden layers*, of which each hidden layer h_t , with $t = 1, \dots, L-2$ is a set of H nodes NH_t .
117 Finally, there is a set of O nodes NO , called *output layer*. Each node (denoted by o) of the output
118 layer is connected with each node (denoted by h) of the NH_{L-2} hidden layer by an edge directed
119 from o to h , and each node y of the NH_1 hidden layer is connected by an edge with each node x of
120 the input layer by an edge directed from y to x .

121 For each edge of the network, we denote by i (resp. j) the source (resp. destination) node and we
122 associate a real value W_{ij} , called *weight*, with the edge.

123 The neural network is used for representing a real function. Each input layer node is associated with
124 an input (real) value and each output layer node is associated with an output (real) value of the
125 function. The output values are computed by the neural network using the input values. Hidden
126 layer nodes are associated with intermediate results of the computation.

127 The neural network computes the output values as follows. Both of each hidden and output layer
128 node n are provided with the same function a , which is called *activation function*, and with a
129 parameter Θ , which is called *bias*. The node j of the first hidden node NH_1 computes its associated

130 hidden value $h_1 = a\left(\sum_{i=1}^I W_{ij} * I_i - \Theta\right)$, where i is an input layer node, i.e., by computing the
131 weighted sum of the values I_i of the input layer using the weights W_{ij} associated with all the
132 connections between each input layer node i and the hidden layer node j .

133 The node j of each hidden layer NH_l computes its associated hidden value

134 $h_j^l = a\left(\sum_{i=1}^H W_{ij} * h_i^{l-1} - \Theta\right)$, where i is the $l-1$ layer node, i.e., by computing the weighted sum of the

135 values h_i^{l-1} of the nodes of the previous layer. Analogously, each output layer node j computes its

136 associated output value $o_j = a\left(\sum_{i=1}^H W_{ij} * h_i^{L-2} - \Theta\right)$, where h_i^{L-2} is a hidden $L-2$ layer node.

137 The weight W_{ij} associated with the edges of the set A and the activation function parameters are

138 suitably set by a *training algorithm* that tries to learn how correctly approximating the desired

139 output. Training algorithms can be unsupervised or supervised. In the first case, the ANN

140 autonomously learns the functional dependence between an input and its correct output. Differently,

141 a supervised training algorithm takes advantage from the availability of a training dataset where for

142 each input its correct output is provided; by measuring the difference between the correct and the

143 computed ANN outputs then it is possible to tune the ANN parameters to minimize this error. When

144 the ANN reaches the desired precision in reproducing the outputs of the training dataset, then the

145 learnt ends and the ANN can be considered ready to work with unknown input data.

146 Multilayer feedforward networks are commonly used to approximate real functions, i.e. for

147 determining weights and parameters of a given neural networks such that a set of given output data

148 matches with a corresponding set of input data, with an approximation error. Some theoretical

149 results have been provided in the related literature (Hetch-Nielsen, 1987) to assure the possibility of

150 approximating any real function satisfying some determined constraints.

151 Many types of activation function a can be used with the above neural network model. In this work,

152 we will use the well-known sigmoid function with the following formula:

153

154
$$a(x) = \frac{I}{1 + e^{-\beta x}} \quad (1)$$

155

156 where β is a parameter that should be appositely chosen when designing the neural network
157 architecture.

158

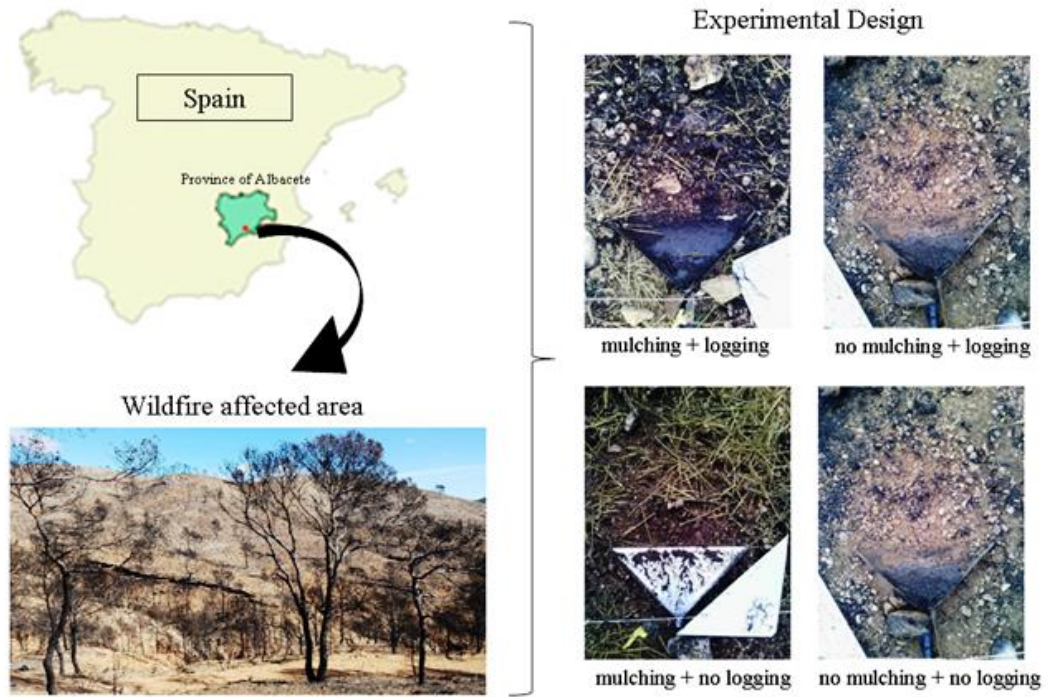
159 3. STUDY AREA

160

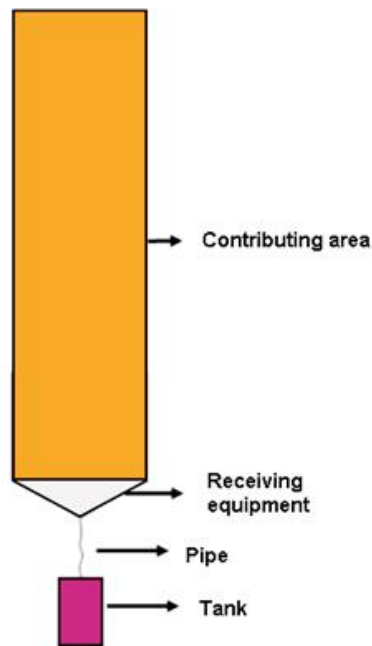
161 The study was carried out in the Sierra de las Quebradas forest (Liétor, Castilla-La Mancha region,
162 province of Albacete, Central Spain) (Figure 1a). The climate is hot dry Mediterranean (Allué,
163 1990), *Bsk* according to the Köppen classification (Kottek et al., 2006). Average annual rainfall and
164 medium annual temperature is 282 mm and 16 °C, respectively. Elevation ranges between 520 and
165 770 m and aspect is W-SW. According to the Spanish Soil Map (2000), soils are classified as
166 *Inceptisols* and *Aridisols* and soil texture is sandy loam.

167 The forest land mainly consists of *Pinus halepensis* M. stands. The mean density and height of
168 forest trees before the wildfire were about 500–650 trees/ha and 7–14 m, respectively. The shrubs
169 and herbaceous species mainly found at the study site were *Rosmarinus officinalis* L.,
170 *Brachypodium retusum* (Pers.) Beauv., *Cistus clusii* Dunal, *Lavandula latifolia* Medik., *Thymus*
171 *vulgaris* L., *Helichrysum stoechas* (L.), *Stipa tenacissima* (L.), *Quercus coccifera* L. and *Plantago*
172 *albicans* L.

173



(a)



(b)

174

175

176 Figure 1 - Location/experimental design (a) and measuring equipment (b) of the experimental plots
 177 used to model the hydrological response of pine forest to wildfire using ANNs (Liétor, Castilla La
 178 Mancha, Spain).

179 **4. METHODS**

180

181 **4.1. Experimental site description**

182

183 Immediately after the wildfire, one site of about five hectares in the forest stand was selected for
184 study (Figure 1a). Twelve experimental plots (each one 9 m long and 3 m wide, for a total area of
185 27 m²) were installed with their longest dimension along the maximum slope in the burned area. In
186 addition, an unburned area, located 7 km far from the burned stand was selected as control and three
187 other plots were located for the same aim.

188 In both areas, the plots were distributed caring that their characteristics (soil properties, slope and
189 aspect) were similar, to ensure comparability. Plot slope varied between 10 and 15%. Plot distance
190 was always higher than 20 m.

191 The plots, delimited by a 0.5 m wide geotextile fabric that was inserted up to 0.4 m below the
192 ground surface, were hydraulically isolated along their perimeter to prevent external inputs of water
193 and sediments. For this, a geotextile that was tightly fastened to 0.8 m long and 20-mm in diameter
194 iron rods was pounded into the ground at 0.15 m of depth. A 50-cm long metallic sediment fence
195 with a triangular shape was installed in the downstream side of the plot, to convey water and
196 sediments in a pipe and then into a 25-litre tank. The area with the metallic fence was protected
197 from rain by a plastic cover. Its ground surface was also covered by plastic, to ensure that the entire
198 runoff and all sediments were delivered to the collection point and then to the storage container
199 (Figure 1b).

200

201 **4.2. Wildfire and forest management operations**

202

203 The Sierra de las Quebradas area was affected in July 2016 by a wildfire. During the wildfire about
204 830 ha of forest land was burned. Tree mortality was 100%. A mean value of soil burn severity was

205 obtained for each plot by adopting the methodology proposed by Vega et al. (2013) and Fernandez
206 et al. (2017). Soil burn severity values were classified in the high class for all of the burned plots by
207 the Castilla La Mancha Forest Service.

208 In September 2016, mulching treatment was carried out in six plots in the burned area. Mulching
209 consisted of manually spreading straw of barley on the plots at a rate of 200 g/m² (dry weight).
210 Initial mulch cover and depth were 95% of the plot area and 3 cm, respectively.

211 Moreover, salvage logging was conducted in December 2016 in six plots, of which three non-
212 mulched and three mulched. The geotextile fabrics of the plots were removed before harvesting and
213 re-installed immediately after. The trees were cut with mechanical chain saws and burned logs were
214 removed using an agricultural tractor equipped with pneumatic wheels.

215 The experimental design consisted of the following *soil conditions* in relation to the wildfire: (1)
216 "*Non-Burned, NB*" (three plots); (2) "*Burned, B*" (twelve plots). After fire the following *soil*
217 *treatments* were defined in the burned plots: (i) *Burned+Mulching+No-Logging (B+M+NL*, six
218 plots); (ii) *Burned+No-Mulching+No-Logging (B+NM+NL*, six plots). This experimental design
219 was adjusted from the cutting date onwards, and the treatments were reassigned as follows: *i*)
220 *Burned+Mulching+Logging (B+M+L*, three plots); *ii*) *Burned-No-Mulching+Logging (B+NM+L*,
221 three plots).

222

223 **4.3. Collection of observed data**

224

225 Precipitation depth, duration and intensity were measured by a weather station (WatchDog 2000
226 Series model) with a tipping bucket rain gauge, located 50 metres out of the study area. In the
227 hourly rainfall series of the experimental database, two consecutive events were considered
228 separate, if no rainfall was recorded for 6 h or more (Wischmeier and Smith, 1978; Zema et al.,
229 2017).

230 Between September 2016 and July 2017, after each precipitation event, the volume of surface
231 runoff collected by the plot tank was measured. After mixing the runoff water collected in the tank,
232 a water sample of about 0.5 litres was collected. Then, samples were oven dried (at 105 °C) for 24 h
233 in the laboratory and Total Dissolved Sediments (TDS) and Suspended Sediments (SS) were
234 measured. Moreover, the eroded soil deposited at each metallic sediment fence was collected
235 manually after each event and then weighed in the field. After sample oven-drying, the dry
236 sediment (DS) weight was measured.

237 The runoff coefficients of each event were calculated as the ratio surface runoff to total rainfall. Soil
238 loss was evaluated as the sum of DS, TDS and SS.

239

240 **4.4. Statistical analysis on observed data**

241

242 Following Lucas-Borja et al. (2019), the observed data were analysed to evaluate the treatment
243 effect (with five levels: *Non-Burned*, *Burned+No-Mulching+No-Logging*, *Burned+Mulching+No-*
244 *Logging*, *Burned+No-Mulching+Logging* *Burned+No-Mulching+No-Logging*) on runoff volumes
245 and soil losses by a general linear mixed model. The survey date and plots were included as random
246 effects. The rainfall parameters (total precipitation, maximum rainfall intensity in 60 min of each
247 rainy event) for each sediment collection date were included as covariates. Data were log-
248 transformed to achieve normality and residuals were tested for autocorrelation, normality and
249 homogeneity of variance. When significant mixed effects were indicated, the post hoc pairwise
250 comparisons (with Bonferroni adjustment for multiple comparisons) were conducted to assess
251 differences between the main effects of treatments and their interactions. All the statistical analyses
252 were conducted using the R statistical program, package lme4.

253

254

255 4.5. ANN implementation

256

257 In these experiments, we used the Neuroph framework for training the ANN on a data set of real
258 hydrological information. The data set contains 243 tuples of four attributes, namely *i*) treatment, *ii*)
259 precipitation (mm), *iii*) runoff (mm) and *iv*) soil loss (kg/ha). Among the input variables, rainfall
260 intensity has not been deliberately included, although many studies (e.g., Lucas-Borja et al., 2019;
261 Prats et al., 2012), carried out in the same environmental conditions, have demonstrated that, beside
262 the total rainfall, rainfall intensity is the most influential variables explaining runoff generation after
263 fire. This choice is due to the fact that many weather stations (as happen in Spain) are equipped
264 only with rain gauges, which provides daily depths rather than with automated devices, allowing
265 continuous measurements of rainfalls for hourly or sub-hourly intensity calculations. By this way,
266 the ANN seems to have a larger transferability compared to the gauged areas.

267 The treatment assumes the following discrete values: *Burned+Mulching+No-Logging*, *Burned+No-*
268 *Mulching+No-Logging*, *Non-Burned*, *Burned+Mulching+Logging* and *Burned+No-*
269 *Mulching+Logging*.

270 The attributes *i*) and *ii*) are considered as the neural network inputs, while *iii*) and *iv*) are used as
271 neural network outputs.

272

273 4.5.1. Data pre-processing

274

275 First, we have processed the data to obtain a suitable dataset to train the neural network. The value
276 of treatment has been transformed into an integer number that takes values between 1 and 5. In
277 particular, *Burned+Mulching+No-logging* = 1, *Burned+No-mulching+No-logging* = 2, *Non-burned*
278 = 3, *Burned+Mulching+Logging* = 4 and *Burned+No-mulching+Logging* = 5. Since some pair of
279 inputs <treatment, precipitation> were associated with different outputs (due to the fact that the
280 same precipitation can produce different runoff volumes, because of many factors, such as the

281 variability of precipitation intensity, soil characteristics in time and space), we averaged in those
 282 cases the values of the surface runoff and soil loss. The new dataset is shown in Table 1a.
 283 Then, the data set had to be normalized. Normalization implies that all values from the dataset
 284 should take values in the range from 0 to 1. For this purpose, we used the following formula:

285

$$286 \quad X_n = \frac{X - X_{min}}{X_{max} - X_{min}} \quad (2)$$

287

288 where X is the value that should be normalized, X_n is the normalized value, X_{min} is the minimum
 289 value of X and X_{max} is the maximum value of X . Therefore, we obtained the dataset shown in Table
 290 1b.

291

292 Tables 1a and 1b - The original (a) and normalized (b) datasets used to model the hydrological
 293 response of plots through ANNs (Liétor, Castilla La Mancha, Spain).

294

295

(a)

Treatment (input 1)	Precipitation (mm) (input 2)	Runoff volume (mm) (output 1)	Soil loss (kg/ha) (output 2)
1.0	40.0	1.65	68.1
2.0	40.0	2.21	316.3
3.0	40.0	0.00	0.0
1.0	41.0	0.41	145.16
2.0	41.0	0.35	403.09
3.0	41.0	0.00	6.366
1.0	59.0	0.25	158.35

2.0	59.0	0.25	424.01
3.0	59.0	0.03	8.3
4.0	93.8	0.60	5.98
5.0	93.8	0.70	77.73
3.0	93.8	0.08	0.6
4.0	28.0	0.15	8.84
5.0	28.0	0.18	19.52
3.0	28.0	0.02	1.97
4.0	16.8	0.13	9.45
5.0	16.8	0.19	15.91
3.0	16.8	0.00	0.0
4.0	11.6	0.02	7.1
5.0	11.6	0.04	38.48
3.0	11.6	0.01	0.79
4.0	47.4	1.46	48.28
5.0	47.4	1.34	103.25
3.0	47.4	0.03	4.15
4.0	20.7	0.08	22.32
5.0	20.7	0.21	21.72
3.0	20.7	0.03	0.26

296

297

298

(b)

Treatment (input 1)	Precipitation (input 2)	Runoff volume (output 1)	Soil loss (output 2)
--------------------------------	------------------------------------	-------------------------------------	---------------------------------

0.0	0.345	0.75	0.16
0.25	0.345	1.0	0.74
0.5	0.345	0.0	0.0
0.0	0.358	0.18	0.34
0.25	0.358	0.16	0.95
0.5	0.358	0.0	0.01
0.0	0.577	0.11	0.37
0.25	0.577	0.11	1.0
0.5	0.577	0.013	0.02
0.75	1.0	0.27	0.01
1.0	1.0	0.32	0.18
0.5	1.0	0.04	0.001
0.75	0.199	0.07	0.02
1.0	0.199	0.08	0.05
0.5	0.199	0.009	0.005
0.75	0.063	0.06	0.02
1.0	0.063	0.08	0.04
0.5	0.063	0.0	0.0
0.75	0.0	0.009	0.02
1.0	0.0	0.018	0.09
0.5	0.0	0.004	0.002
0.75	0.435	0.66	0.114
1.0	0.435	0.6	0.24
0.5	0.435	0.013	0.0097
0.75	0.111	0.04	0.53

1.0	0.111	0.095	0.51
0.5	0.111	0.013	6.0e ⁻⁰⁴

299

300

301 Tables 2a and 2b - Runoff volume (a) and soil loss (b) observed and simulated by the ANN used to
 302 model the hydrological response of plots through (Liétor, Castilla La Mancha, Spain).

303

304

(a)

Observed runoff (mm)	Simulated runoff (mm)	Error (mm)
1.65	1.65	0
2.21	2.14	0.07
0	0.025	0.025
0.41	0.39	0.02
0.35	0.35	0
0	0.0084	0.0084
0.25	0.243	0.007
0.25	0.21	0.04
0.03	0.06	0.03
0.6	0.57	0.03
0.7	0.7	0
0.08	0.11	0.03
0.15	0.15	0
0.18	0.21	0.03
0.02	0.0097	0.0103

0.13	0.085	0.045
0.19	0.13	0.06
0	0.007	0.007
0.02	0.072	0.052
0.04	0.11	0.07
0.01	0.0075	0.0025
1.46	1.46	0
1.34	1.33	0.01
0.03	0.00044	0.02956
0.08	0.1	0.02
0.21	0.15	0.06
0.03	0.0075	0.0225

305

306

(b)

Observed soil loss (kg/ha)	Simulated soil loss (kg/ha)	Error (kg/ha)
68.1	85.18	17.08
316.3	320.42	4.12
0	0.38	0.38
145.16	136.49	8.67
403.09	401.96	1.13
6.36	0.42	5.94
158.35	157.69	0.66
424.01	424.01	0
8.3	12.42	4.12

5.98	0.975	5.005
77.73	76.19	1.54
0.6	2.03	1.43
8.84	7.93	0.91
19.52	20.35	0.83
1.97	0.38	1.59
9.45	11.45	2
15.91	24.8	8.89
0	0.72	0.72
7.1	14.96	7.86
38.48	30.4	8.08
0.79	1.02	0.23
48.28	48.76	0.48
103.25	101.93	1.32
4.15	3.985	0.165
22.32	9.54	12.78
21.72	21.88	0.16
0.26	0.55	0.29

307

308

309 *4.5.2. Neural network architecture*

310

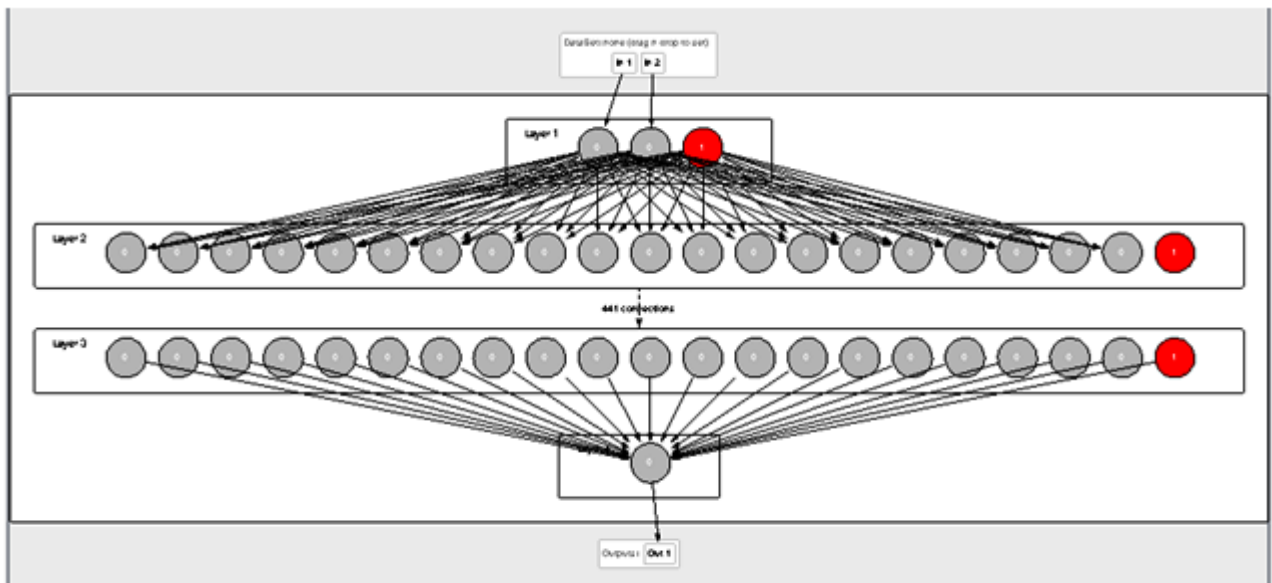
311 We adopted the Neuroph, which is an ANN tool, and the *Multi Layer Perceptron* architecture,
 312 which is a feedforward ANN (see Section 2). This ANN model maps sets of input data into a set of
 313 appropriate output. It consists of multiple layers of nodes in a directed graph, with each layer fully

314 connected to the next one. Except for the input nodes, each node is a neuron with nonlinear
315 activation function.

316 Multilayer perceptron uses a supervised learning technique called *backpropagation* for the training
317 stage. It is a modification of the standard linear Perceptron, which is not able to distinguish data that
318 not linearly separable, as in our case. We set multi-layer perceptron's parameters. The number of
319 input and output neurons was the same as in the training set. Then, we had to choose number of
320 hidden layers, and number of neurons in each layer.

321 The topology of our ANN was chosen as the result of a preliminary study, where several
322 alternatives in terms of number of hidden layers and number of neurons for layer were tested. At the
323 end of this study, the best performance architecture resulted in two hidden layers with 20 neurons in
324 each layer (Figure 2).

325



326

327 Figure 2 - The ANN with two hidden layers with 20 following neurons used to model the
328 hydrological response of plots (Liétor, Castilla La Mancha, Spain).

329

330

331 Then we adopted a 'Sigmoid' for transfer function, while, for learning rule, we chose a
332 'Backpropagation with Momentum'. The momentum is a real value added to speed up the process of
333 learning and to improve the efficiency of the algorithm.

334

335 4.5.3. Neural network training

336

337 After we have created training set and set the parameters of the neural network, we started to train
338 it. When the *Total Net Error* value dropped below the max error, the training was complete. The
339 smaller the error is, the better the obtained approximation is.

340 In our case the maximum error was set to 0.0001, learning rate was set to 0.2 and momentum was
341 set to 0.7. In the first phase, we calculated the total Mean Square Error (MSE). For that purpose, the
342 following formula was used:

343

$$344 \quad MSE = \frac{1}{n} \sum_{i=1}^n (Y_i - \hat{Y}_i)^2 \quad (3)$$

345

346 where MSE is the arithmetic mean of the squares of the errors $(Y_i - \hat{Y}_i)^2$.

347 To have a global view of the error, the Mean Absolute Error (MAE) was calculated using the
348 following formula:

349

$$350 \quad MAE = \frac{1}{n} \sum_{i=1}^n |A_t - F_t| \quad (4)$$

351

352 where A_t are the actual output and F_t corresponding predictions.

353

354

355 **4.6. Evaluation of the hydrological prediction capability of ANN**

356

357 The predictions of surface runoff and soil loss provided by the adopted ANN model were compared
358 to the corresponding observations collected in the equipped plots. First, observed and simulated
359 values were visually compared in "scatter-plots". Then, the following indicators, usually adopted in
360 the literature studies dealing with hydrological modelling (e.g., Willmott, 1982; Legates and
361 McCabe, 1999; Loague and Green, 1991; Zema et al., 2017; 2018), were calculated:

- 362 (i) the main statistics (i.e. the maximum, minimum, mean and standard deviation of both the
363 observed and simulated values);
- 364 (ii) the coefficients of determination (r^2), efficiency (E, Nash and Sutcliffe, 1970) and residual
365 mass (CRM, also known as "percent bias", PBIAS); and
- 366 (iii) the Root Mean Square Error (RMSE).

367 The related equations for the calculation of these indicators are reported by Zema et al. (2012),
368 Krause et al. (2005), Moriasi et al. (2007) and Van Liew and Garbrecht (2003).

369 To summarise, the model performance can be evaluated as follows:

- 370 - the closer the statistics, the more accurate the model predictions;
- 371 - values of r^2 , ranging from 0 to 1, over 0.5 indicate reasonable model performance (Santhi et al.,
372 2001; Van Liew et al., 2003; Vieira et al., 2018);
- 373 - E, in the range $-\infty$ to 1, is negative for a model giving poor predictions, ≥ 0.35 for a satisfactory
374 model and ≥ 0.75 for a good performance (Zema et al., 2017);
- 375 - RMSE, which should be as closest as possible to zero (no errors between predictions and
376 observations), less than half the standard deviation of the measured data are considered good
377 (Singh et al., 2004);
- 378 - CRM/PBIAS, which, if positive, indicates model underestimation, whereas, if negative, model
379 overestimation (Gupta et al., 1999), must be below 0.25 or 0.55 for good runoff and soil loss
380 predictions, respectively, according to Moriasi et al. (2007).

381

382 **5. RESULTS AND DISCUSSIONS**

383

384 **5.1. Runoff and soil erosion observations**

385

386 During the observation period, nine events were monitored, for which precipitation depth and mean
387 intensity were in the range 11.6-93.8 mm and 0.98-28.0 mm/h. The monitored events were only
388 those producing surface runoff and erosion. As expected, all burned plots gave runoff volumes and
389 soil loss significantly (at $p < 0.05$) much higher than non-burned soils (control), for which the mean
390 runoff and soil loss were 0.02 ± 0.03 mm and 2.49 ± 3.07 kg/ha (mean \pm standard deviation). Also
391 Gimeno-García et al. (2007), studying the soil's hydrological response after wildfires in
392 Mediterranean shrublands, showed that total runoff and sediment yield in the first post-fire year
393 (19.43 mm and 0.56 kg/m^2 in the intense fire) contrast with the very low runoff (3.82 mm) and soil
394 loss (0.08 kg/m^2) in control plots. In a different Mediterranean landscape, Mayor et al (2007) found
395 that total runoff and sediment yield in the burned catchment (35 mm and 4.56 kg/ha, respectively)
396 were considerably greater than in the unburned catchment (0.03 mm, and 0.12 kg/ha). Key casual
397 factors enhancing runoff and soil loss are the reduction in infiltration and some combination of
398 sealing, soil water repellency, loss of surface cover, and disaggregation due to loss of soil organic
399 matter (Neary et al., 2005).

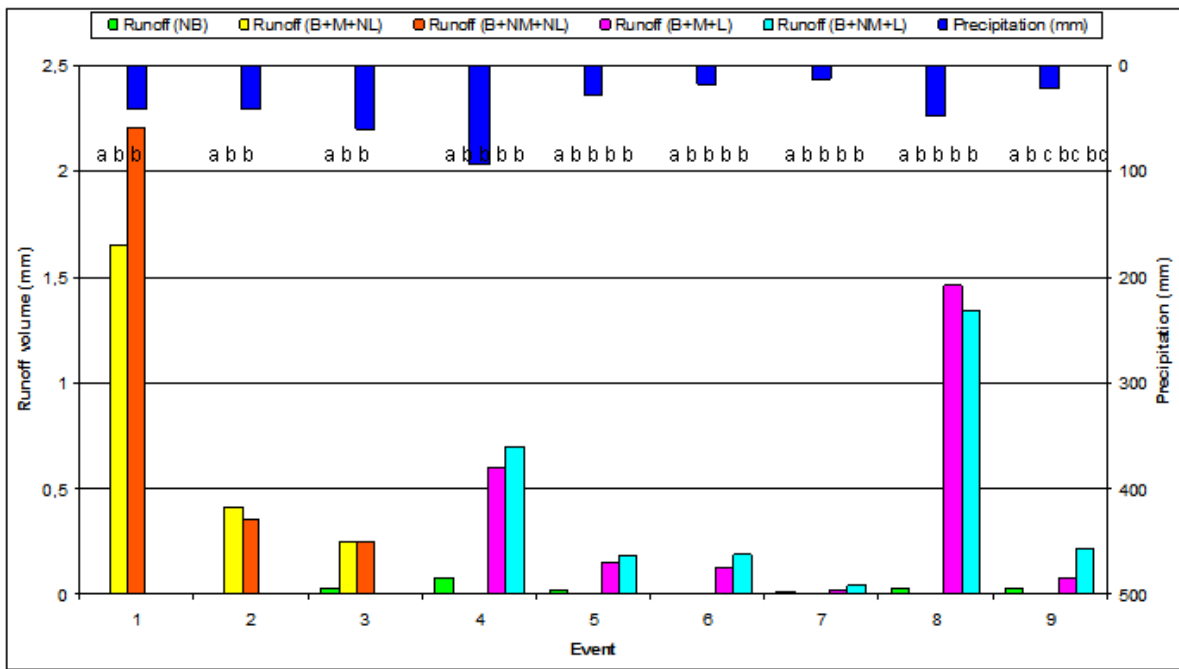
400 Mulching reduced the hydrological response of the burned and non-logged soils (mean runoff of
401 0.26 ± 0.54 mm as well as soil loss of 41.3 ± 66.6 kg/ha soils) compared to non-mulched plots
402 (runoff of 0.31 ± 0.72 mm and soil loss of 127 ± 193 kg/ha) (Figure 3a and 3b). The differences
403 were significant for soil erosion, but not for runoff. The efficacy of mulch application to control
404 soil erosion is in accordance with Bautista et al. (2009), who highlighted the immediate increase of
405 ground cover in mulch application, which result in an effective soil protection for the first rain
406 events after fire.

407 The effects of logging on burned soils (mulched or not) anywhere not appreciably different between
408 the plots., since the differences in surface runoff and soil loss were not significant (at $p < 0.05$).
409 More specifically, non-mulched plots gave higher runoff (0.30 ± 0.45) and soil loss (30.7 ± 36.7
410 kg/ha) compared to soils treated with straw (mean runoff of 0.27 ± 0.48 mm and soil loss of $11.3 \pm$
411 15.5 kg/ha) (Figure 3a and 3b). This is in accordance with other authors that did not report a
412 significantly negative effect of logging in soil parameters (Fernández and Vega, 2016). The type of
413 machinery used during forest operations could also explain this. As Lucas-Borja et al. (2018)
414 demonstrated, the use of not heavy machinery with air tires generates not negative impact on soil
415 and reduce soil compaction in comparison to chain tires.

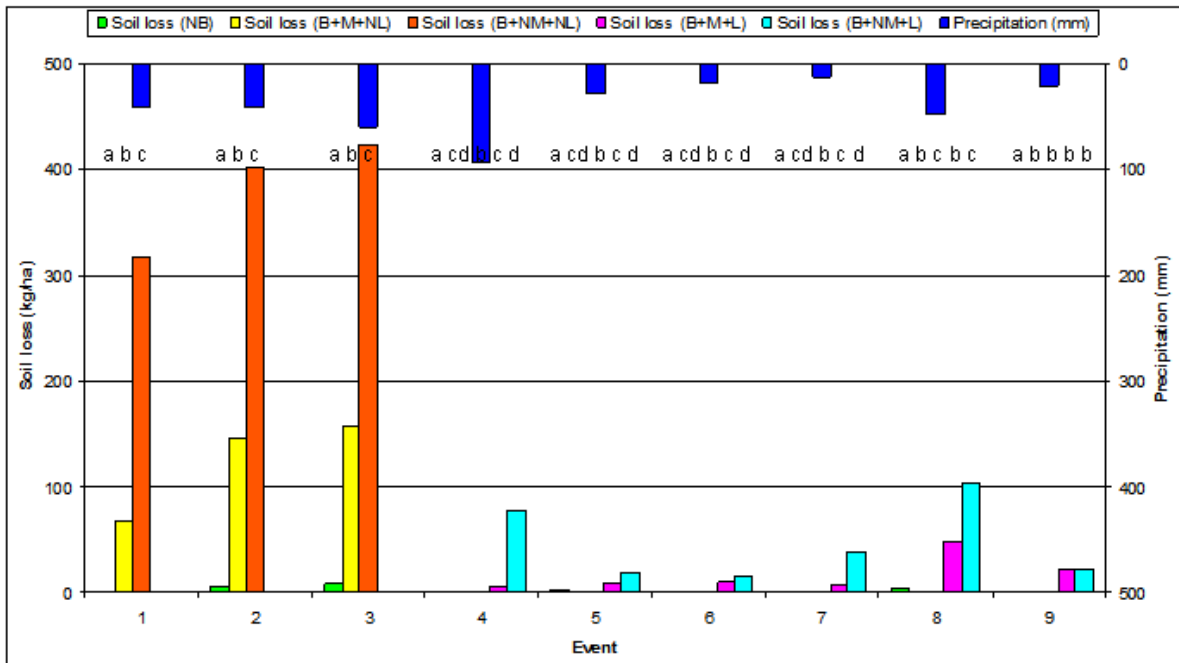
416 It is worth to highlight that a temporal gradient in runoff generation mechanism was found for the
417 burned and non-logged plots, regardless of the treatment, indicating a decrease of the hydrological
418 response of all soils throughout the time elapsed from fire. In other words, the largest runoff - and
419 thus soil loss - was produced by the rainfall events occurring immediately after the wildfire, as
420 shown by the decrease of the runoff coefficients (data not shown). This has been observed in the
421 first and second storms in the season immediately after wildfires by several authors (e.g., de Dios
422 Benavides-Solorio and MacDonald, 2005; DeBano et al., 1998; MacDonald et al., 2000; Robichaud
423 and Brown, 1999). The large increase in the runoff coefficients just after fire has been attributed to
424 changes in soil hydrological properties, such as the development of a water-repellent layer at or near
425 the soil surface, which prevents infiltration and induces overland flow (DeBano et al., 1970;
426 Shakesby et al., 2000). In addition, this fact might be explained by the vegetation (mainly shrubs
427 and herb) recovery after fires that performed better than litter in order to stop runoff generation. The
428 complex system of vegetation patches in control plots which is highly disconnected that influence
429 of semiarid Mediterranean vegetation on runoff generation has been widely reported in previous
430 studies (i.e. Dunjó et al., 2004).

431

432



(a)



(b)

433

434 Figures 3a and 3b - Precipitation, runoff volumes (a) and soil losses (b) observed in the
 435 experimental plots (Liétor, Castilla La Mancha, Spain) (NB = Non-Burned; B+M+NL =
 436 Burned+Mulching+No-Logging; B+NM+NL = Burned+No-Mulching+No-Logging; B+M+L =

437 Burned+Mulching+Logging; B+NM+L = Burned+No-Mulching+Logging; different lower case
438 letters indicate statistically significant differences at $p < 0.05$).

439

440 **5.2. Hydrological modelling by ANN**

441

442 First, we train the neural network for the first output. After 250000 iterations we obtained a Total
443 Network Error (equal to the Total Mean Square Error) drop down to a specified level of 0.0001,
444 which means that training process was successful.

445

446 *5.2.1. Neural Network Approximation*

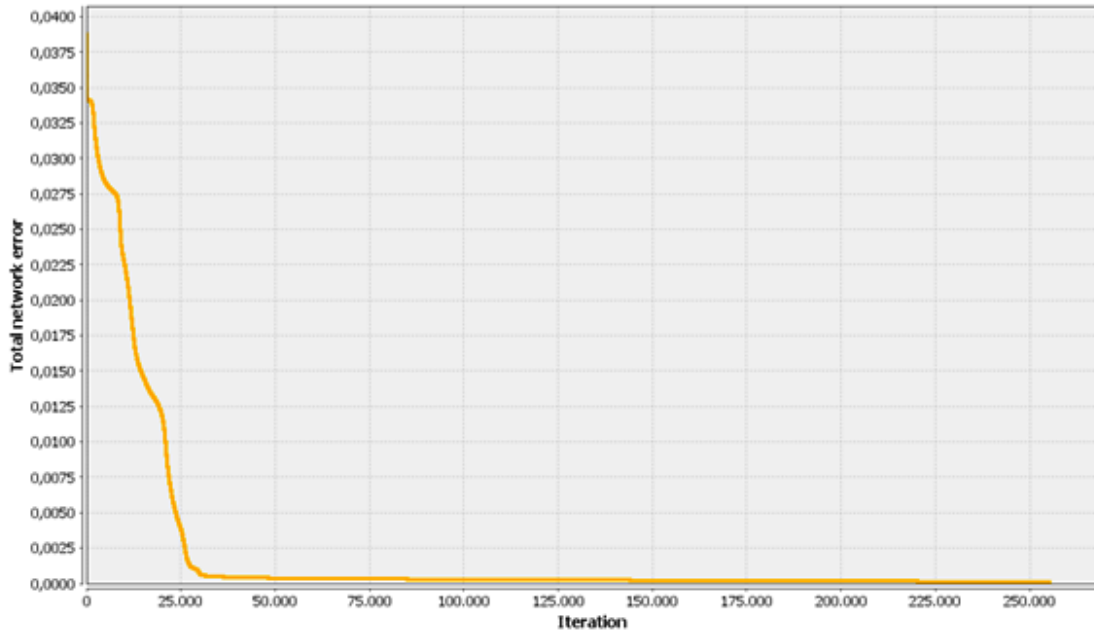
447

448 A Total Mean Square Error of 1.965×10^{-4} in simulating the runoff volume was achieved (Figure 4a),
449 which certainly is a very good result, because our goal is to get the total error to be as small as
450 possible. In more detail, Table 2a reports the observed (desired output) and simulated (ANN output)
451 runoff values and the related differences the trained neural network produced. Looking at the
452 individual errors, we can observe that most of them are at the low level, below 0.1. MAE was equal
453 to 0.025 mm. So we can conclude that this type of neural network architecture is the best choice.

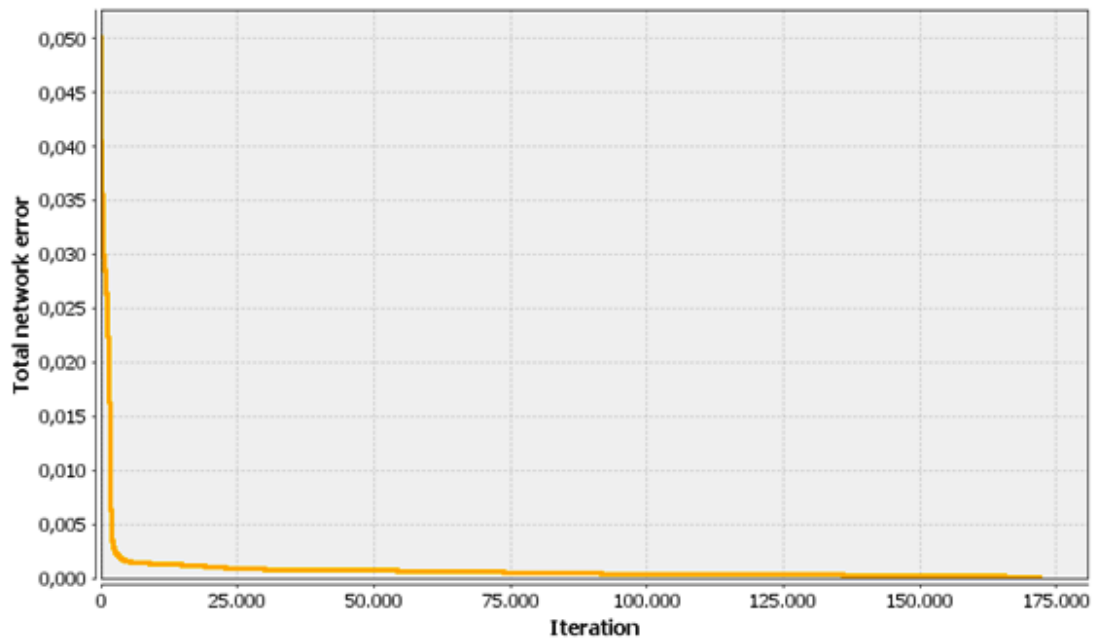
454 We used the same neural network shown in Figure 2. Also in this case, we set the maximum error to
455 0.0001, the learning rate to 0.2 and the momentum to 0.7. After 175000 iterations we obtained a
456 total Total Network Error (MSE) drop down to a specified level of 0.0001, which means that
457 training process was successful and that now we can exploit this trained neural network (Figure 4b).
458 The Total Mean Square Error for this second neural network was 1.78×10^{-4} . The relative error on the
459 individual soil loss between the observations and the simulations (Table 2b) was lower than 17.1
460 kg/ha while MAE was equal to 3.57 kg/ha.

461

462



(a)



(b)

463

464 Figures 4a and 4b - Total Network Error (equal to the Total MSE, Mean Square Error) for runoff

465 volume (a) and soil loss (b) simulated by the ANN used to model the hydrological response of plots

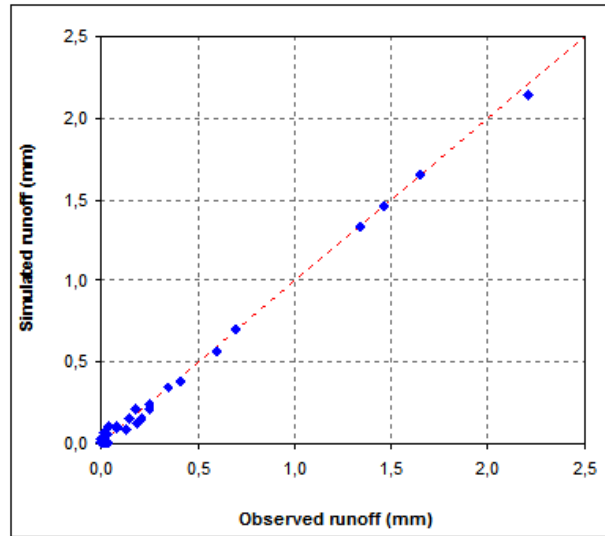
466 (Liétor, Castilla La Mancha, Spain).

467

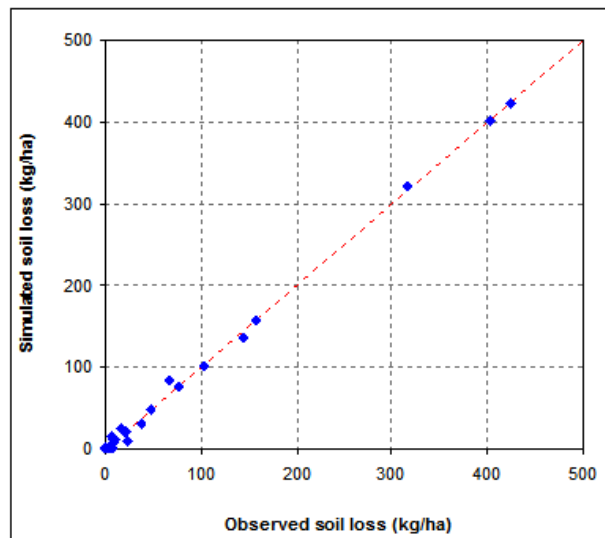
468 5.2.2. Evaluation of the ANN prediction capability

469

470 The scatter plots of Figure 5a and 5b show a very close agreement between the predictions provided
471 by ANN and the corresponding observations collected at the plots for both surface runoff volumes
472 and soil loss for all the experimental conditions (control, burned and treated/not treated soils).



(a)



(b)

473

474

475 Figures 5a and 5b - Scatter plot of the observed vs simulated (by ANN) runoff volumes (a) and soil
476 loss (b) in the experimental plots (Liétor, Castilla La Mancha, Spain).

477

478 This qualitative agreement is confirmed by the values of the indicators adopted for the quantitative
479 assessment of ANN prediction capability. In general, when the ANN performance is evaluated by
480 aggregating all the soil conditions, the statistics (i.e., mean, standard deviation, minimum and
481 maximum) were practically equal for both runoff and soil loss. Only very small differences were
482 found for the maximum runoff (under 3.2%) and the minimum soil loss (modelled as zero against a
483 mean value of 0.38 kg/ha). Moreover, the model efficiency and RMSE are good and the coefficient
484 of determination equal to one, while the CRM (equal to 0.01) indicates a very small model
485 underestimation of the observations (Table 3).

486 A more detailed analysis of the ANN performance, carried out separately for the individual soil
487 conditions (burned/unburned) and treatments (mulching/logging) highlighted that (Table 3):

488 - the observed and predicted mean values of both runoff and soil loss are practically the same and
489 the maximum difference (16.2%, however under the acceptance threshold) is detected for soil loss
490 prediction in B+M+L plots;

491 - the lower agreement between observations and predictions was found in the maximum runoff
492 (with differences lower than 32%) and in the minimum soil loss (below 112%); for the latter, in
493 same cases the ANN predicted soil losses equal to zero also in the case of observed erosion; instead,
494 for the maximum soil losses, only in one case (for the B+M+L plots) the difference with the
495 corresponding observation was more than 20%.

496 Table 3 - Values of the criteria adopted for ANN evaluation in the experimental plots (Liétor, Castilla La Mancha, Spain).

497

Treatment	Number of events	Value	Mean	Minimum	Maximum	Standard Deviation	E	CRM	r ²	RMSE
RUNOFF VOLUME										
<i>ALL DATA</i>	27	Observed	0.39	0.00	2.21	0.59	-	-	-	-
		Simulated	0.38	0.00	2.14	0.58	1.00	0.01	1.00	0.03
<i>NB</i>	9	Observed	0.57	0.00	2.21	0.80	-	-	-	-
		Simulated	0.56	0.01	2.14	0.78	1.00	0.01	1.00	0.03
<i>B+M+NL</i>	3	Observed	0.46	0.08	0.70	0.33	-	-	-	-
		Simulated	0.46	0.11	0.70	0.31	0.99	0.00	1.00	0.02
<i>B+NM+NL</i>	3	Observed	0.12	0.02	0.18	0.09	-	-	-	-
		Simulated	0.12	0.01	0.21	0.10	0.93	-0.06	0.99	0.02
<i>B+M+L</i>	6	Observed	0.07	0.00	0.19	0.08	-	-	-	-
		Simulated	0.07	0.01	0.13	0.05	0.55	-0.06	0.56	0.05
<i>B+NM+L</i>	6	Observed	0.53	0.03	1.46	0.68	-	-	-	-
		Simulated	0.51	0.00	1.46	0.69	1.00	0.03	1.00	0.03

SOIL LOSS										
ALL DATA	27	Observed	70.96	0.00	424.01	120.84	-	-	-	-
		Simulated	70.99	0.38	424.01	120.96	1.00	0.00	1.00	5.60
NB	9	Observed	169.96	0.00	424.01	170.74	-	-	-	-
		Simulated	171.00	0.38	424.01	170.21	1.00	-0.01	1.00	6.98
<i>B+M+NL</i>	3	Observed	196.89	8.30	424.01	210.52	-	-	-	-
		Simulated	198.04	12.42	424.01	208.74	1.00	-0.01	1.00	2.41
<i>B+NM+NL</i>	3	Observed	10.11	1.97	19.52	8.84	-	-	-	-
		Simulated	9.55	0.38	20.35	10.08	0.97	0.06	1.00	1.16
<i>B+M+L</i>	6	Observed	11.96	0.00	38.48	14.26	-	-	-	-
		Simulated	13.89	0.72	30.40	12.15	0.79	-0.16	0.82	5.93
<i>B+NM+L</i>	6	Observed	33.33	0.26	103.25	38.25	-	-	-	-
		Simulated	31.11	0.55	101.93	38.85	0.98	0.07	0.98	5.25

498 Notes: NB = Non-Burned; B+M+NL = Burned+Mulching+No-Logging; B+NM+NL = Burned+No-Mulching+No-Logging; B+M+L =

499 Burned+Mulching+Logging; B+NM+L = Burned+No-Mulching+Logging.

500 As regards the other model performance indicators, the following considerations can be drawn
501 (Table 3):

502 - ANN showed a very slight tendency to overestimate or underestimate the hydrological
503 observations (for instance, overestimation of runoff in B+NM+L and B+NM+L plots, CRM = -0.06
504 as well as underestimation of soil loss in B+NM+NL and B+NM+L, CMR = 0.06-0.07), as shown
505 by the very small negative or positive values of CMR;

506 - for all the soil conditions/treatments and both for runoff and soil loss predictions, E, r^2 and RMSE
507 attained good values (that is, very close to one for E and r^2 , and to zero for RMSE), except for the
508 B+M+L plots;

509 - for the latter soil condition and treatment, the worst performance of the ANN was found for both
510 runoff and erosion predictions (see values of E, r^2 and RMSE). Presumably, in soil subjected to
511 logging, the impacts of machinery wheels on soil determine the formation of small rills, in which
512 small volumes of water and sediments are stored and do not feed runoff. Since, in general, many
513 models find difficulties in modelling rill erosions (e.g., Aksoy and Kavvas, 2005), this behaviour
514 could be common with ANN.

515 However, on account of E, r^2 and RMSE values, the prediction capability of the ANN can be
516 considered as satisfactory to good for runoff and good for soil loss. This indicates that a soil
517 disturbance due to more than two factors (in our case wildfire, mulching and logging) finds some
518 difficulties in being simulated by ANN, which however does not compromise the generally good
519 model performances.

520 The runoff and erosion prediction capacity provided by ANNs appears to be very satisfactory in the
521 experimental conditions and this is even more appreciable if we make comparisons with other
522 conceptual models. For instance, limiting the evaluation criteria to model efficiency, the very high
523 E coefficients of this study (close to 0.99) is noticeably higher compared to the maximum values (E
524 from -10 to 0.93) reported in the studies of Vieira et al. (2014), Fernandez et al. (2010) and Hosseini
525 et al. (2018), who applied the MMF model for predicting runoff and erosion at seasonal and annual

526 scales on soils of Iberian Peninsula, burned by fires of different severity and subjected to different
527 post-fire treatments. Fernandez et al. (2010) and Fernandez and Vega (2016) found some
528 inaccuracies of the RUSLE model (shown by a negative E) for predicting annual soil erosion from
529 burned soils of NW Spain, since the K factor did not allow to reflect the changes on soil
530 permeability and structure after fire, while the annual soil loss predictions achieved by Vieira et al.
531 (2018) applying RUSLE in north-central Portugal were more satisfactory ($E = 0.63-0.70$).
532 Contrasting results in annual erosion prediction capacity provided by PESERA model applied in
533 burned plots were shown by coefficients E of 0.33 (Fernandez and Vega, 2016) or 0.73-0.85 (Vieira
534 et al., 2018).

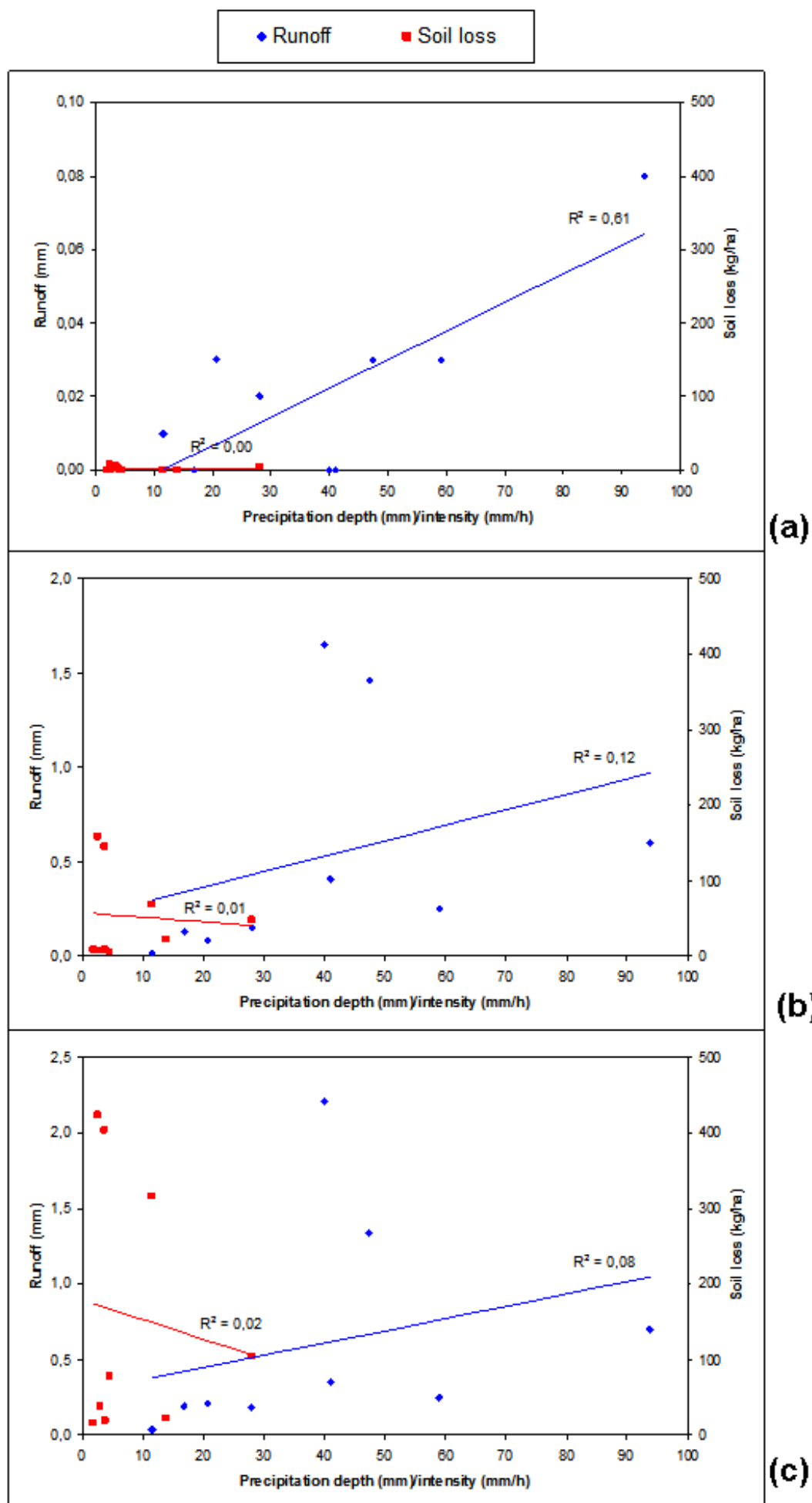
535 The ANN models focus on mathematical solutions over process representation, such as the
536 empirical models do. In other words, it is a “black box” approach, which estimates runoff and soil
537 loss, but does not gives information about the physical factors underlying the hydrological
538 processes. Nonetheless, empirical models are frequently used in preference to more complex
539 models as they can be implemented in situations with limited data and parameter inputs, and are
540 particularly useful as a first step in identifying sources of water, sediments and pollutants (Merritt et
541 al., 2003). However, the main goal of technicians and land planners is first the knowledge of the
542 runoff and erosion rates and then the selection of the most suitable treatment to reduce the
543 unsustainable rates, rather than a detailed comprehension of the hydrological processes. For
544 stakeholders or government agencies, who may be responsible for land and water management on a
545 national or regional basis, the complex models are prohibitive in terms of the time required to
546 develop and implement them (Fu et al., 2018). Since the data requirements of any model increase
547 with the model complexity, models that are less complex than the physically-based models, such as
548 the empirical models (Aksoy and Kavvas, 2005), are more indicated for use in burned areas of
549 Mediterranean forests, which are often data-poor environments. Low-data demanding models are
550 based primarily on the analysis of observations and seek to characterise response from these data
551 (Wheater et al., 1993). The simplest models are regression equations between climatic variables

552 (such as precipitation volumes and intensities) and runoff/erosion rates. However, in the
553 experimental areas, linear regressions were not able to predict with accuracy runoff volumes and
554 soil loss from simple observations of precipitation. As a matter of fact, very low coefficients of
555 determination were found by regressing both runoff volumes and soil loss to precipitation depth and
556 intensity in non-burned soils as well as in burned plots (mulched or not) (Figure 6). This
557 presumably happened, since these simple models ignore the inherent non-linearities in the
558 hydrological processes and employ unrealistic assumptions about the physics (Wheater et al., 1993).
559 Conversely, the ANNs, which require only precipitation as input, but use a more complex
560 mathematical structure, were successful in capturing the output hydrological variables from the
561 observational input data, as shown by the very good prediction capacity detected for the ANNs in
562 the experimental conditions of this study.

563 Therefore, the main advantages of the ANN use are in such environmental contexts are the low
564 input requirement in comparison to the more complex physically-based models and, at the same
565 time, the prediction accuracy in comparison to the simpler empirical models. This is appreciated by
566 land planners and forest managers, who have a powerful prediction tool easy to be used in data-poor
567 environment, as often the Mediterranean forests are.

568 Overall, the use of ANNs for hydrological predictions in burned areas of Mediterranean forests
569 appears to be suitable, since this modelling approach only needs precipitation data (whose
570 measuring equipments are available also in forestlands) as well as a reasonable set of rainfall-runoff
571 observations to train the ANN.

572



574 Figure 6 - Linear regression between runoff volumes and precipitation depth as well as soil loss and
575 maximum 1-h precipitation intensity in the experimental non-burned (a), burned and mulched (b)
576 and burned and non-mulched (c) plots (Liétor, Castilla La Mancha, Spain).

577

578

579 **6. CONCLUSIONS**

580

581 The evaluation of the ANN for hydrological modelling in the forest plots subject to wildfire showed
582 that the runoff and erosion prediction capability is in general very good. The ANN performance was
583 exceptionally high for all the experimental conditions, since the model efficiency and the coefficient
584 of determination was equal to one, while the very low CRM indicated a negligible underestimation
585 of the observations. The ANN proposed is also very robust, in the sense that its performance is
586 exceptionally high for all the experimental conditions (burned or non-burned soils) and treatments
587 (mulching and/or logging or not), with only one exception (that is, in the condition where the soil
588 disturbance is higher). Thus, the potential applicability of the ANN is promising as management
589 tool for predicting and controlling the hydrogeological risk in Mediterranean forest ecosystems
590 threatened by wildfire as well as for evaluating the efficiency of post-fire treatments. Moreover, this
591 approach is more desirable compared to the most complex physically-based models or the less
592 accurate empirical equations, since ANNs require low amount of data, but, at the same time, offer a
593 good prediction capacity of hydrological variables.

594 However, further experimental tests are needed to assure ANN applicability to these climatic,
595 geomorphological and ecological contexts and to upscale the model applications from the plot to the
596 watershed scale. On the other hand, a larger and general use of ANN for hydrological predictions
597 requires more experimental investigations in other environmental contexts (different for climate and
598 geomorphology), which should assure a large transferability of this modelling tool for hydrological
599 and ecological management in forest ecosystems potentially prone to fire.

600 If simulations of runoff and erosion remain good also out of the experimental conditions of this
601 study after fire, the availability of powerful ANNs can support landscape planners not only in
602 control the fire risk in forestland, but also in identifying the most efficient countermeasures to limit
603 ecosystem degradation. Conversely, in the case of less accurate hydrological predictions, other
604 important variables - of easy measurement or estimation, - influencing the runoff and erosion
605 generation mechanisms should be implemented when an ANN is designed, such as the rainfall
606 intensity, vegetal cover and texture of soils. Therefore, estimations of water flows and soil erosion
607 using ANN decrease the costs and the studies time otherwise required by hydrological models of
608 other nature.

609 Overall, the study aims to consolidate the use of ANNs - a well-known efficient technique of
610 Artificial Intelligence - as decision support system for the integrated assessment and management of
611 forested watersheds.

612

613 **REFERENCES**

614

615 Aksoy, H. and Kavvas, M.L., 2005. A review of hillslope and watershed scale erosion and sediment
616 transport models. *Catena* 64(2-3), 247-271.

617 Albaradeyia, I., Hani, A., Shahrour, I., 2011. WEPP and ANN models for simulating soil loss and
618 runoff in a semi-arid Mediterranean region. *Environmental monitoring and assessment* 180(1-4),
619 537-556.

620 Allué, J.L., 1990. Atlas fitoclimático de España. Taxonomías. Ministerio de Agricultura, Pesca y
621 Alimentación. INIA Madrid, Spain.

622 Asadi, H., Shahedi, K., Jarihani, B., Sidle, R.C., 2019. Rainfall-runoff modelling using hydrological
623 connectivity index and artificial neural network approach. *Water* 11(2), 212.

624 ASCE Task Committee, 2000. Artificial neural networks in hydrology. I. Preliminary concepts. *J*
625 *Hydraul Eng ASCE* 5(2), 115–123.

626 Bautista, S., Robichaud, P.R., Bladé, C., 2009. Post-fire mulching. *Fire Eff. Soils Restor. Strateg.*
627 *Sci. Publ. Enfield, NH.* 353–372.

628 Benavides-Solorio, J.D. and Macdonald, L.H., 2005. Measurement and prediction of post-fire
629 erosion at the hillslope scale, Colorado Front Range. *International Journal of Wildland Fire* 14, 457-
630 474.

631 Certini, G., 2014. Fire as a soil-forming factor. *Ambio* 43, 191–195.

632 Dawson, C.W. and Wilby, R., 1998. An artificial neural network approach to rainfall-runoff
633 modelling. *Hydrological Sciences Journal* 43(1), 47-66.

634 Esteves, T.C.J., Kirkby, M.J., Shakesby, R.A., Ferreira, A.J.D., Soares, J.A.A., Irvine, B.J.,
635 Fernández, C., Vega, J.A., Vieira, D.C.S., 2010. Assessing soil erosion after fire and rehabilitation
636 treatments in NW Spain: performance of RUSLE and revised Morgan–Morgan–Finney
637 models. *Land degradation & development* 21(1), 58-67.

638 Fernández, C. and Vega, J.A., 2016. Evaluation of RUSLE and PESERA models for predicting soil
639 erosion losses in the first year after wildfire in NW Spain. *Geoderma* 273, 64–72..

640 Ferreira, C.S.S., Coelho, C.O.A., Bento, C.P.M., Carreiras, M.A., 2012. Mitigating land degradation
641 caused by wildfire: application of the PESERA model to fire affected sites in central Portugal.
642 *Geoderma* 191, 40-50.

643 Fu, B., Merritt, W.S., Croke, B.F., Weber, T., Jakeman, A.J., 2018. A review of catchment-scale
644 water quality and erosion models and a synthesis of future prospects. *Environmental modelling &*
645 *software* 114, 85-97.

646 Gholami, V., Booij, M.J., Tehrani, E.N., Hadian, M.A., 2018. Spatial soil erosion estimation using
647 an artificial neural network (ANN) and field plot data. *Catena* 163, 210-218.

648 Gimeno-García E., Andreu V., Rubio J.L., 2007. Influence of vegetation recovery on water erosion
649 at short and medium-term after experimental fires in a Mediterranean shrubland. *Catena* 69, 150-
650 160.

651 Haykin S. , 1994. *Neural Networks: A Comprehensive Foundation*. Prentice Hall, USA.

652 Hetch-Nielsen, R., 1987. Kolmogorov's mapping neural network existence theorem. In Proceedings
653 of the International Conference on Neural Networks, vol. 3, 11-14, New York, USA.

654 Hosseini, M., Nunes, J. P., Pelayo, O. G., Keizer, J.J., Ritsema, C., Geissen, V., 2018. Developing
655 generalized parameters for post-fire erosion risk assessment using the revised Morgan-Morgan-
656 Finney model: A test for north-central Portuguese pine stands. *Catena* 165, 358-368.

657 Hsu, K.-L., Gupta, H.V., Sorooshian, S., 1995. Artificial neural network modeling in rainfall–runoff
658 process. *Water Resources Research* 31(10), 2517–2530.

659 Kim, M. and Gilley, J.E., 2008. Artificial Neural Network estimation of soil erosion and nutrient
660 concentrations in runoff from land application areas. *Computers and electronics in
661 agriculture* 64(2), 268-275.

662 Kottek, M., Grieser, J., Beck, C., Rudolf, B., Rubel, F., 2006. World Map of the Köppen-Geiger
663 climate classification updated. *Meteorol. Z.* 15, 259-263.

664 Larsen, I.J., MacDonald, L.H., Brown, E., Rough, D., Welsh, M.J., Pietraszek, J.H., Schaffrath, K.,
665 2009. Causes of post-fire runoff and erosion: water repellency, cover, or soil sealing? *Soil Science
666 Society of America Journal* 73(4), 1393-1407.

667 Legates, D.R. and McCabe, G.J., 1999. Evaluating the use of “goodness of fit” measures in
668 hydrologic and hydroclimatic model validation. *Water Resources Research* 35, 233-241.

669 Licznar, P. and Nearing, M.A., 2003. Artificial neural networks of soil erosion and runoff
670 prediction at the plot scale. *Catena* 51(2), 89-114.

671 Loague, K. and Green, R.E., 1991. Statistical and graphical methods for evaluating solute transport
672 models: Overview and application. *Journal of Contaminant Hydrology* 7, 51-73.

673 Lucas-Borja, M.E., Plaza-Álvarez, P.A., Gonzalez-Romero, J., Sagra, J., Alfaro-Sánchez, R., Zema,
674 D.A., de Las Heras, J., 2019. Short-term effects of prescribed burning in Mediterranean pine
675 plantations on surface runoff, soil erosion and water quality of runoff. *Science of The Total
676 Environment* 674, 615-622.

677 Lucas-Borja, M.E., González-Romero, J., Plaza-Álvarez, P.A, Sagra, J., Gómez M.E., Moya, D.,
678 Cerdà, A., de las Heras, J., 2018. The impact of straw mulching and salvage logging on post-fire
679 runoff and soil erosion generation under Mediterranean climate conditions. *Science of the Total*
680 *Environment* 654, 441-451.

681 Lucas-Borja, M.E., Zema, D.A., Carrà, B.G., Cerdà, A., Plaza-Alvarez, P.A., Cózar, J.S., de las
682 Heras, J., 2018. Short-term changes in infiltration between straw mulched and non-mulched soils
683 after wildfire in Mediterranean forest ecosystems. *Ecological Engineering* 122, 27-31.

684 Mayor, A.G., Bautista, S., Llovet, J., Bellot, J., 2007. Post-fire hydrological and erosional responses
685 of a Mediterranean landscape: Seven years of catchment-scale dynamics. *Catena* 71, 68–75.

686 Merritt, W.S., Letcher, R.A., Jakeman, A.J., 2003. A Review of Erosion and Sediment Transport
687 Model. *Environmental Modelling and Software* 18, 761-799

688 Moody, J.A., Shakesby, R.A., Robichaud, P.R., Cannon, S. H., Martin, D.A., 2013. Current
689 research issues related to post-wildfire runoff and erosion processes. *Earth-Science Reviews* 122,
690 10-37.

691 Morales, H.A., Navar, J., Dominguez, P.A., 2000. The effect of prescribed burning on surface
692 runoff in a pine forest stand of Chihuahua, Mexico. *Forest Ecol Manag* 137, 199–207

693 Moriasi, D.N., Arnold, J.G., Van Liew, M.W., Bingner, R.L., Harmel, R.D., Veith, T.L., 2007.
694 Model evaluation guidelines for systematic quantification of accuracy in watershed
695 simulations. *Transactions of the ASABE* 50 (3), 885-900.

696 Nash, J.E. and Sutcliffe, J.V., 1970. River flow forecasting through conceptual models: Part I. A
697 discussion of principles. *Journal of Hydrology* 10, 282-290.

698 Neary, D.G., Ryan, K.C., DeBano, L.F., 2005. Wildland fire in ecosystems: effects of fire on soils
699 and water. Gen. Tech. Rep. RMRS-GTR-42-vol. 4. Ogden, UT US Dep. Agric. For. Serv. Rocky
700 Mt. Res. Station. 250 p. 42.

701 Plaza-Álvarez, P.A., Lucas-Borja, M.E., Sagra, J., Zema, D.A., González-Romero, J., Moya, D., De
702 las Heras, J., 2019. Changes in soil hydraulic conductivity after prescribed fires in Mediterranean
703 pine forests. *Journal of Environmental Management* 232, 1021-1027.

704 Prats, S.A., MacDonald, L.H., Monteiro, M., Ferreira, A.J., Coelho, C.O., Keizer, J.J., 2012.
705 Effectiveness of forest residue mulching in reducing post-fire runoff and erosion in a pine and a
706 eucalypt plantation in north-central Portugal. *Geoderma* 191, 115-124.

707 Prats, S.A., MacDonald, L.H., Monteiro, M., Ferreira, A.J.D., Coelho, C.O.A., Keizer, J.J., 2012.
708 Effectiveness of forest residue mulching in reducing post-fire runoff and erosion in a pine and a
709 eucalypt plantation in north-central Portugal. *Geoderma* 191, 115–124.

710 Riad, S., Mania, J., Bouchaou, L., Najjar, Y., 2004. Rainfall-runoff model using an artificial neural
711 network approach. *Mathematical and Computer Modelling* 40(7-8), 839-846.

712 Robichaud, P.R., Elliot, W.J., Pierson, F.B., Hall, D.E., Moffet, C.A., Ashmunm L.E., 2007.
713 Erosion risk management tool (ERMiT) user manual, version 2006.01.18. US Department of
714 Agriculture, Forest Service, Rocky Mountain Research Station, General Technical Report RMRS-
715 GTR- 188., Fort Collins, Colorado. USA.

716 Robichaud, P.R., 2000. Fire effects on infiltration rates after prescribed fire in Northern Rocky
717 Mountain forests, USA. *Journal of Hydrology* 231, 220-229.

718 Santhi, C., Arnold, J.G., Williams, J.R., Dugas, W.A., Srinivasan, R., Hauck, L.M., 2001.
719 Validation of the SWAT model on a large river basin with point and nonpoint sources. *J. Am.*
720 *Water Resour. Assoc.* 37 (5), 1169–1188.

721 Shakesby, R.A., 2011,. Post-wildfire soil erosion in the Mediterranean: review and future research
722 directions. *Earth-science reviews*, 105(3-4), 71-100.

723 Sharma, S.K. and Tiwari, K.N., 2009. Bootstrap based artificial neural network (BANN) analysis
724 for hierarchical prediction of monthly runoff in Upper Damodar Valley Catchment. *Journal of*
725 *hydrology* 374(3-4), 209-222.

726 Singh, J., Knapp, H.V., Demissie, M., 2004. Hydrologic modeling of the Iroquois River watershed
727 using HSPF and SWAT. ISWS CR 2004-08. Champaign, Ill.: Illinois State Water Survey.
728 <http://www.sws.uiuc.edu/pubdoc/CR/ISWSCR2004-08.pdf> (Accessed 14 February 2018).

729 Sudheer, K.P., Gosain, A.K., Ramasastri, K.S., 2002. A data-driven algorithm for constructing
730 artificial neural network rainfall-runoff models. *Hydrological processes* 16(6), 1325-1330.

731 Tokar, A.S. and Johnson, P.A., 1999. Rainfall runoff modeling using artificial neural networks.
732 *Journal of Hydrologic Engineering* 4 (3), 232–239.

733 Van Liew, M.W., Arnold, J.G., Garbrecht, J.D., 2003. Hydrologic simulation on agricultural
734 watersheds: choosing between two models. *Trans. ASAE* 46 (6), 1539–1551.

735 Van Liew, M.W and Garbrecht, J., 2003. Hydrologic simulation of the Little Washita River
736 experimental watershed using SWAT. *Journal of the American Water Resources Association*

737 Vega, J.A., Fernández, C., Fontúrbel, M.T., González-Prieto, S.J., Jiménez, E., 2014. Testing the
738 effects of straw mulching and herb seeding on soil erosion after fire in a gorse shrubland. *Geoderma*
739 223–225, 79–87.

740 Vega, J.A., Fontúrbel, M.T., Merino, A., Fernández, C., Ferreiro, A., Jiménez, E., 2013. Testing the
741 ability of visual indicators of soil burn severity to reflect changes in soil chemical and microbial
742 properties in pine forests and shrubland. *Plant and Soil* 369, 73–91.

743 Vieira, D.C.S., Prats, S.A., Nunes, J.P., Shakesby, R.A., Coelho, C.O.A., Keizer, J.J., 2014.
744 Modelling runoff and erosion, and their mitigation, in burned Portuguese forest using the revised
745 Morgan-Morgan-Finney model. *For. Ecol. Manag.* 314, 150–165.

746 Vieira, D.C.S., Serpa, D., Nunes, J.P.C., Prats, S.A., Neves, R., Keizer, J.J., 2018. Predicting the
747 effectiveness of different mulching techniques in reducing post-fire runoff and erosion at plot scale
748 with the RUSLE, MMF and PESERA models. *Environmental Research* 165, 365-378.

749 Wheater, H.S., Jakeman, A.J., Beven, K.J., 1993. Progress and directions in rainfall-runoff
750 modelling. In: Jakeman, A.J., Beck, M.B., McAleer, M.J. (Eds.), *Modelling Change in*
751 *Environmental Systems*. John Wiley and Sons, Chichester, USA, 101-132.

752 Willmott, C.J., 1982. Some comments on the evaluation of model performance. *Bulletin of*
753 *American Meteorological Society* 63(11), 1309-1313.

754 Wischmeier, W.H. and Smith, D.D. (1978) *Predicting Rainfall Erosion Losses: A Guide to*
755 *Conservation Planning*. Science, US Department of Agriculture Handbook, No. 537, Washington
756 DC, USA.

757 Yusof, M.F., Azamathulla, H.M., Abdullah, R., 2014. Prediction of soil erodibility factor for
758 Peninsular Malaysia soil series using ANN. *Neural Computing and Applications* 24(2), 383-389.

759 Zema, D.A., Bingner, R.L., Govers, G., Licciardello, F., Denisi, P., Zimbone, S.M., 2012.
760 Evaluation of runoff, peak flow and sediment yield for events simulated by the AnnAGNPS model
761 in a Belgian agricultural watershed. *Land Degradation and Development* 23(3): 205-215.

762 Zema, D.A., Labate, A., Martino, D., Zimbone, S.M., 2017. Comparing Different Infiltration
763 Methods of the HEC-HMS Model: The Case Study of the Mésima Torrent (Southern Italy). *Land*
764 *Degradation & Development* 28(1), 294-308.

765 Zema, D.A., Lucas-Borja, M.E., Carrà, B.G., Denisi, P., Rodrigues, V.A., Ranzini, M., Zimbone, S.
766 M., 2018. Simulating the hydrological response of a small tropical forest watershed (Mata
767 Atlantica, Brazil) by the AnnAGNPS model. *Science of the Total Environment* 636, 737-750.